AIP | Applied Physics Letters

Ultrafast optical image processing based on third-harmonic generation in organic thin films

Canek Fuentes-Hernandez, Shuo-Yen Tseng, Daniel Owens, and Bernard Kippelen

Citation: Appl. Phys. Lett. **91**, 131110 (2007); doi: 10.1063/1.2790826
View online: http://dx.doi.org/10.1063/1.2790826
View Table of Contents: http://apl.aip.org/resource/1/APPLAB/v91/i13
Published by the American Institute of Physics.

Related Articles

Using filtering effects to identify objects
Chaos 22, 023107 (2012)

Super-resolution spatial frequency differentiation of nanoscale particles with a vibrating nanograting
Appl. Phys. Lett. 100, 011101 (2012)

Fractal descriptors in the Fourier domain applied to color texture analysis
Chaos 21, 043112 (2011)

A wavelet transform algorithm for peak detection and application to powder x-ray diffraction data
Rev. Sci. Instrum. 82, 015105 (2011)

Support vector machine-based feature extractor for L/H transitions in JET
Rev. Sci. Instrum. 81, 10E123 (2010)

Additional information on Appl. Phys. Lett.

Journal Homepage: http://apl.aip.org/
Journal Information: http://apl.aip.org/about/about_the_journal
Top downloads: http://apl.aip.org/features/most_downloaded
Information for Authors: http://apl.aip.org/authors

ADVERTISEMENT

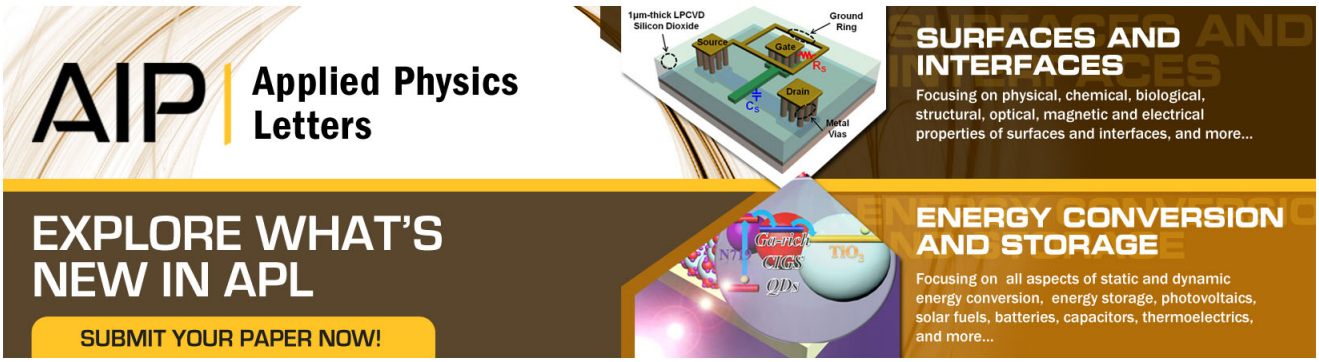

Ultrafast optical image processing based on third-harmonic generation in organic thin films

Canek Fuentes-Hernandez, Shuo-Yen Tseng, Daniel Owens, and Bernard Kippelen[a)]
Center for Organic Photonics and Electronics, School of Electrical and Computer Engineering, Georgia Institute of Technology, Atlanta, Georgia 30332, USA

(Received 18 July 2007; accepted 8 September 2007; published online 26 September 2007)

We report on the use of the noncollinear third-harmonic generation in an amorphous polymer film operating in the eye safe and telecommunication compatible near-infrared range to perform ultrafast all-optical two-dimensional (2D) image processing at 1550 nm using 100 fs pulses. The background-free and nondegenerate outputs at 517 nm are easily spatially filtered and detected with low cost electronic components. We describe this Fourier transform based technique and demonstrate its application to the classical problem of 2D image recognition. © *2007 American Institute of Physics*. [DOI: 10.1063/1.2790826]

Due to their massive intrinsic parallelism, optical systems are attractive for applications that require computationally intensive operations. The problem of two-dimensional (2D) image processing is a good example where optical systems offer such advantages. When these systems are implemented using ultrafast nonlinear optical (NLO) processes, computational rates faster than 10^{16} operations/s could be achieved.[1] In comparison, BlueGene/L, the fastest supercomputer today, can perform 2.8×10^{14} floating point operations/s.[2] The constant advances in ultrafast laser technologies and NLO material research continue to bring ultrafast optical processing closer to its realization. Third-harmonic generation (THG) is an inherently ultrafast electronic process that has already found many applications in laser frequency conversion,[3] characterization of ultrafast pulses,[4] microscopy,[5,6] and imaging through scattering media.[5,6] To date, most THG applications pertained to the characterization of ultrafast pulses through temporal autocorrelation, because third-order processes allow full access to the amplitude and phase information of a pulse without direction-of-time ambiguity.[7] Recently, we demonstrated the use of an amorphous polymer composite with strong THG at telecommunication wavelengths for the characterization of subnanojoule femtosecond pulses by interferometric autocorrelation[8] and by frequency-resolved optical gating.[9] Ballistic-photon imaging through scattering media using ultrafast gating was also demonstrated.[10] In this letter, we expand the range of applications for THG processes by demonstrating Fourier-transform-based 2D optical image processing using noncollinear THG at 1550 nm. In contrast with the previously proposed ultrafast optical image processors that use a Kerr media in a phase-conjugated geometry,[1] the forward-folded crossed-beam phase-matched coherent anti-Stokes Raman spectroscopy (BOXCARS) geometry used for the noncollinear THG process can be implemented in a very compact setup using a diffractive optical element (DOE) to generate the input beams and assure their spatial and temporal overlap.[11] Even though the BOXCARS geometry has been used in the past for degenerate four-wave mixing (DFWM) imaging experiments,[12] the THG correlator produces signal outputs that are nondegenerate, background-free, and spatially separated in the visible spectral range. Thus, they can be spatially filtered with an iris and are not affected by scattering at the fundamental wavelength. Scattering is a particularly difficult problem to deal with in DFWM experiments, in particular, if hundreds of micrometer thick samples are required to produce signals that are strong enough to be detected with current charge coupled device (CCD) technologies sensitive in the telecommunication range. In contrast, the THG signals produced by a 10 μm thick polymer composite sample are strong enough to be seen by the naked eye and easily detected with low-cost Si-based electronic components that do not require image intensifiers.

This noncollinear THG approach is based on a joint transform correlator configuration implemented through a 4-*f* imaging system, as shown in Fig. 1. The optical system simultaneously receives three linearly polarized and collimated pulses at frequency ω. The spatial field distribution of each pulse is modulated in transmission or reflection by amplitude masks that contain, respectively, the 2D images of the desired impulse response $h(\mathbf{r})$, the data to be filtered $g(\mathbf{r})$, and the reconstruction wave $r(\mathbf{r})$. The amplitude masks are placed at the front focal plane of lens 1 and Fou-

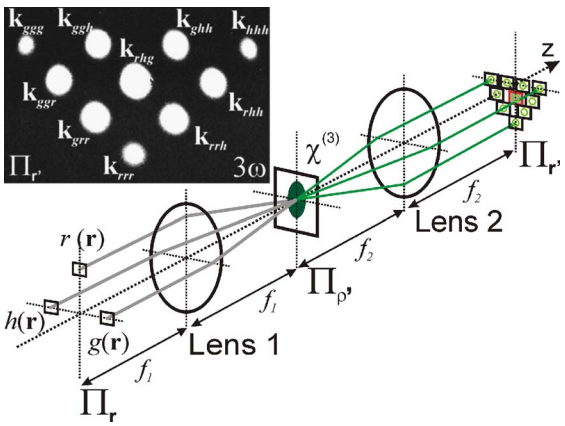

FIG. 1. (Color online) Schematics of the joint transform correlator geometry used for the implementation of the noncollinear THG correlator. The inset shows the ten THG beams generated when three noncollinear pulses coincide spatially and temporally in the NLO material along with the fundamental wave vector combinations that give rise to them.

[a)]Electronic mail: kippelen@gatech.edu

rier transformed into the NLO material at its back focal plane, where the angular spectra of the 2D images are multiplied through the material third-order NLO susceptibility, $\chi^{(3)}(3\omega;\omega,\omega,\omega)$ [hereafter denoted by $\chi^{(3)}$]. In this three-beam noncollinear THG configuration, the interacting beams with wave vectors $\mathbf{k}_h(\omega)$, $\mathbf{k}_g(\omega)$, and $\mathbf{k}_r(\omega)$ will give rise to ten different optical fields at frequency 3ω. The direction of each beam is determined by one of the possible combinations of the three wave vectors at ω, $\mathbf{k}_{ijk}(3\omega)=\mathbf{k}_i(\omega)+\mathbf{k}_j(\omega)+\mathbf{k}_k(\omega)$ (with i, j, $k=h$, g, r), see, the inset of Fig. 1. This configuration takes full advantage of (i) the nonphase matched and (ii) the third-order nature of the THG process by avoiding the spatial overlap of beams that contain different information. Of particular interest for 2D optical image processing applications is the central beam propagating in the direction $\mathbf{k}_{rhg}(3\omega)$, which at the NLO material can be approximated as

$$E_{RHG}\left(\frac{\boldsymbol{\rho}}{\lambda f_1};3\omega\right)\propto\chi^{(3)}R\left(\frac{\boldsymbol{\rho}}{\lambda f_1};\omega\right)H\left(\frac{\boldsymbol{\rho}}{\lambda f_1};\omega\right)G\left(\frac{\boldsymbol{\rho}}{\lambda f_1};\omega\right), \tag{1}$$

where capital letters denote the Fourier transforms of the respective 2D images, λ is the fundamental wavelength, and f_1 is the focal length of lens 1. After propagating through lens 2, with focal length f_2, the spatial distribution at the back focal plane of lens 2, the output plane, will have the form

$$\varepsilon_{rhg}\left(\frac{3f_1}{f_2}\mathbf{r};3\omega\right)\propto\chi^{(3)}r\left(\frac{3f_1}{f_2}\mathbf{r}\right)\otimes h\left(\frac{3f_1}{f_2}\mathbf{r}\right)\otimes g\left(\frac{3f_1}{f_2}\mathbf{r}\right), \tag{2}$$

where $\otimes$ denotes the convolution operation. Note that the frequency conversion process demagnifies the original images because the third-harmonic field propagates with a reduced wavelength ($\lambda_{THG}=\lambda/3$) which rescales its angular spectrum by a factor of 3. Nevertheless, the total magnification can be controlled by a proper selection of the magnification factor f_2/f_1. Since the output field distribution is directly proportional to the convolution of the input fields, using a delta function for the reconstruction wave $r(\mathbf{r})=\delta(\mathbf{r})$, returns an output that is proportional to the convolution: $h(\mathbf{r})\otimes g(\mathbf{r})$, while the cross correlation can be accessed by inverting the impulse response around its origin, $h(\mathbf{r})\star g(\mathbf{r})=h(-\mathbf{r})\otimes g(\mathbf{r})$.[13] The other noncollinear THG beams will produce spatially separated outputs that can be equally accessed at the output plane. Such field distributions are of the type $f(\mathbf{r})\otimes f(\mathbf{r})$ in the directions $\mathbf{k}_{rff}(3\omega)$, and $f(\mathbf{r})\otimes\delta(\mathbf{r})$ in the directions $\mathbf{k}_{rrf}(3\omega)$, with $f(\mathbf{r})=h(\mathbf{r})$, $g(\mathbf{r})$. Similar noncollinear THG geometries have been used in the past to perform temporal autocorrelations for the characterization of femtosecond pulses[14,15] and to demonstrate all-optical full logic units.[16]

The 4-f imaging system was implemented using 2 in. diameter singlet planoconvex spherical lenses with a 10 cm focal length. Spatial and temporal overlap of the three interacting pulses were achieved by using a DOE beam splitter which eliminated the need for temporal delay lines. A detailed description of this setup can be found in Ref. 11. Transmission binary masks printed on overhead transparencies were used as images to modulate the input beams. Each beam was focused into the sample with an external angle of 5.7° with respect to the optical axis. A maximum resolution of 14.3 lines/mm, limited by spherical aberration, was determined at the fundamental wavelength using a standard USAF resolution target. The NLO medium was the polymer composite reported in Refs. 8–10, which contains the molecule *E*-2-tricyanovinyl-3-*n*-hexyl-5-[4-bis(4-nbutylphenyl)-amino-2-methoxy-styryl]thiophene[17] doped at a 20 wt % loading into a polystyrene matrix. Using spectral ellipsometric measurements at the third-harmonic wavelength (517 nm) and prism coupler measurements at the fundamental wavelength (1550 nm), a wave vector mismatch of $|\Delta\mathbf{k}|=0.168\ \mu m^{-1}$ was measured for the collinear THG process in this material, which is smaller than previously estimated.[8,18] For the noncollinear THG process, the angular separation of the pulses reduces $\Delta\mathbf{k}$ and makes the THG process more efficient in those directions, as seen in Fig. 1. While the conversion efficiency reaches a maximum at external angles of around 20° with respect to the optical axis,[18] such large angles lead to stringent aberration requirements and the implementation of the correlator, a problem of optical design which is beyond the scope of this work. The coherence length of the THG process in this material was then estimated to be $\pi/|\Delta\mathbf{k}|=9.2\ \mu m$. Accordingly, a 10 μm thick film was prepared as previously described.[8] An ultrafast optical parametric amplifier (Newport TOPAS) pumped by a Ti:sapphire regenerative amplifier (Newport Spitfire) producing 100 fs pulses at 1550 nm with a repetition rate of 1 kHz was used in our experiments. Before the transmission masks, an energy of 2.8 μJ/pulse was measured. The signal of interest at the third harmonic was spatially filtered with an iris, and captured with a low cost Si-based CCD camera (Genwac, GW-902H).

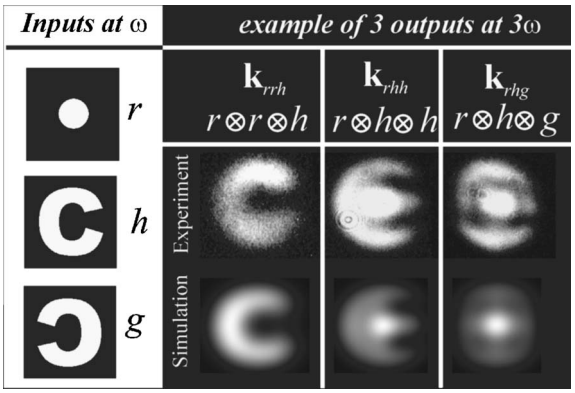

FIG. 2. Output images on three different positions of the output plane using the input 2D binary images indicated on the left of the table. The other figures demonstrate access to imaging through frequency conversion: $r\otimes r\otimes h$, convolution: $r\otimes h\otimes h$, and cross correlation: $r\otimes h\otimes g$ captured in the $\mathbf{k}_{rrh}$, $\mathbf{k}_{rhh}$, and $\mathbf{k}_{rgh}$ directions. MATLAB simulations of the operations indicated in each column performed on the 2D binary images used for the experiment are shown for comparison.

Without the binary masks, ten noncollinear THG beams are clearly observed at the output plane of the correlator providing evidence of the good spatial and temporal overlap of the pulses (see Fig. 1). To illustrate the intensity distributions that can be recovered at the output plane of the correlator, we have introduced the character "C," approximately $3.5\times3.5\ mm^2$, in two different orientations as $h=h(\mathbf{r})$ and $g=h(-\mathbf{r})$, and a 1.5 mm aperture as $r(\mathbf{r})$ in the reconstruction arm. As shown in Fig. 2, simultaneous access to imaging through frequency conversion: $r\otimes r\otimes h$, convolu-

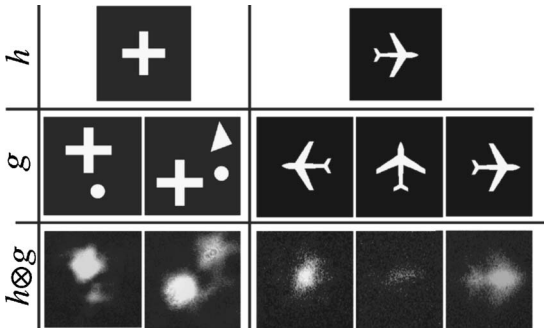

FIG. 3. Correlator output in the $\mathbf{k}_{hgr}$ direction, demonstrating image recognition: of a cross against some geometrical images and of an airplane for different orientations, demonstrating the expected sensitivity of the convolution operation to object rotations.

tion: $r \otimes h \otimes h$, and cross correlation: $r \otimes h \otimes g$ operations are obtained in the directions: $\mathbf{k}_{rrh}, \mathbf{k}_{rhh}$, and $\mathbf{k}_{rgh}$ respectively. Using a simple MATLAB routine, the intensity distributions $|\varepsilon_{rjk}(\mathbf{r}')|^2$ were modeled by numerically applying the corresponding operations to the binary images used in the experiment. As expected, the finite extent of the reconstruction wave produces a smoothing effect on the images, acting as a low-pass filter at the sample position by controlling the extent of the angular spectrum that is efficiently recovered through the THG process. Image recognition can then be implemented using this correlator scheme. As shown in Fig. 3, positive identification of a cross surrounded by other geometrical objects was achieved. Furthermore, we performed recognition experiments of a more complex object using an airplane and showed the expected sensitivity of the convolution operation to object rotations and that stronger signals are obtained through the autocorrelation operation.[13] For the airplane recognition experiments, we have used a reference aperture of 0.5 mm to improve the resolution over the previous experiments.

In summary, using 100 fs pulses at 1550 nm, we have presented a proof-of-principle demonstration of ultrafast all-optical processing in an amorphous NLO polymer composite through a noncollinear THG technique. We foresee that improvements in the optical setup could allow operating this correlator with unamplified femtosecond pulses in the nanojoule range, as well as significantly improving the spatial resolution. Even with the limitations of our current setup, assuming that the smallest resolvable feature is 0.5 mm, the size of the minimum aperture used in our experiments, two images of 14×14 elements could be correlated within a time of 100 fs. Thus, this correlator is capable of performing at least 3.9×10^{15} operations/s in the $\mathbf{k}_{rgh}$ direction. The nonphase matched nature of the THG process allows for this polymer composite to be used from 1400 to 1800 nm,[10] which potentially could admit wavelength multiplexing capabilities to this approach. Even though the lack of ultrafast spatial light modulators is for now the true bottle neck for the realization of ultrafast optical processing technologies, the possibility of achieving real-time holographiclike capabilities through a technique that is ultrafast, nondegenerate, and easily implemented in a robust and compact setup compatible with low-cost electronic components could make this noncollinear THG correlation technique an attractive alternative for technologies requiring real-time optical processing capabilities, which so far may have been limited by the slow response times of typical holographic materials.

The authors would like to thank Professor S. R. Marder and his group for providing the organic NLO chromophore for the THG experiments, Professor J. Perry and the members of his group for giving us time to work with their laser system, and Professor J. Goldhar and Dr. W. N. Herman for providing the DOE used for the implementation of the correlator. This work was funded in part by NSF through STC DMR-0120967 and by DARPA through the MORPH program under contract No. N00014-04-1-0095.

[1] C. Halvorson, A. Hays, B. Kraabel, R. L. Wu, F. Wudl, and A. J. Heeger, Science **265**, 1215 (1994).
[2] See http://www.llnl.gov/asc/computing_resources/bluegenel/ for further details.
[3] R. W. Boyd, *Nonlinear Optics*, 1st ed. (Academic, San Diego, CA, 1992), p. 4.
[4] J. C. M. Diels, J. J. Fontaine, I. C. Mcmichael, and F. Simoni, Appl. Opt. **24**, 1270 (1985).
[5] A. Kuditcher, B. G. Hoover, M. P. Hehlen, E. N. Leith, S. C. Rand, and M. P. Shih, Appl. Opt. **40**, 45 (2001).
[6] Y. Barad, H. Eisenberg, M. Horowitz, and Y. Silberberg, Appl. Phys. Lett. **70**, 922 (1997).
[7] E. I. Blount and J. R. Klauder, J. Appl. Phys. **40**, 2874 (1969).
[8] G. Ramos-Ortiz, M. Cha, S. Thayumanavan, J. C. Mendez, S. R. Marder, and B. Kippelen, Appl. Phys. Lett. **85**, 179 (2004).
[9] G. Ramos-Ortiz, M. Cha, S. Thayumanavan, J. Mendez, S. R. Marder, and B. Kippelen, Appl. Phys. Lett. **85**, 3348 (2004).
[10] G. Ramos-Ortiz, M. Cha, B. Kippelen, G. A. Walker, S. Barlow, and S. R. Marder, Opt. Lett. **29**, 2515 (2004).
[11] S.-Y. Tseng, C. Fuentes-Hernandez, and B. Kippelen, Opt. Lett. **32**, 2599 (2007).
[12] P. Ewart, P. G. R. Smith, and R. B. Williams, Appl. Opt. **36**, 5959 (1997).
[13] J. W. Goodman, *Introduction to Fourier Optics*, 2nd. ed. (MacGraw-Hill, San Francisco, CA, 1996), p. 396.
[14] M. Samoc, A. Samoc, and B. Luther-Davies, Opt. Express **11**, 1787 (2003).
[15] T. M. Liu, Y. C. Huang, G. W. Chern, K. H. Lin, Y. C. Hung, C. J. Lee, and C. K. Sun, IEEE J. Quantum Electron. **38**, 1529 (2002).
[16] R. P. Schmid, T. Schneider, and J. Reif, Opt. Commun. **207**, 155 (2002).
[17] S. Thayumanavan, J. Mendez, and S. R. Marder, J. Org. Chem. **64**, 4289 (1999).
[18] G. Ramos-Ortiz, Ph.D. thesis, University of Arizona, 2003.